Bull. Mater. Sci., Vol. 39, No. 7, December 2016, pp. 1843–1850. © Indian Academy of Sciences.
DOI 10.1007/s12034-016-1327-3

Physicochemical, structural and induced ferromagnetic properties of Co–In-codoped CdO synthesised via Cd chloride: significant effect of post-treatment hydrogen

A A DAKHEL* and W E ALNASER
Department of Physics, College of Science, University of Bahrain, P.O. Box 32038, Bahrain, Kingdom of Bahrain

MS received 26 February 2016; accepted 4 May 2016

Abstract. **Nanoparticle solid solution powders of cadmium oxide doped with different concentrations of cobalt and indium ions were synthesised by solvothermal method through $CdCl_2{\cdot}H_2O$ precursor route. The objective of the present work is to study and develop conditions necessary to create stable room-temperature ferromagnets (RT-FMs) in transparent conducting oxide (TCO) CdO for applications in the field of dilute magnetic semiconductors (DMSs). To achieve this aim, cobalt (Co^{2+}) dopant ions were used as a source of stable FM, while In^{3+} dopant ions supply free electrons that enhance the electronic medium of interaction. The electronic medium in the host CdO lattice, which carries the long-range spin–spin (*S.S*) exchange interaction between localised Co^{2+} (3d) spins of dopant ions, was further developed by annealing in hydrogen gas (hydrogenation). The crystalline structure of the powder samples was investigated by the X-ray diffraction (XRD) method. The optical absorption properties were studied by diffuse reflection spectroscopy (DRS). Magnetic measurements reveal that the Co–In-codoped CdO powder has FM properties superimposed on paramagnetic (PM) behaviour. However, annealing in hydrogen atmosphere strongly boosts the created FM so that the saturation magnetisation increases ∼90 times. Physical explanations and discussion are given in the article. Thus, it is proved that the magnetic properties could be tailored to TCO CdO by Co-doping and post-treatment under H_2 atmosphere.**

Keywords. **Co–In-codoped CdO; room-temperature ferromagnetism; hydrogen treatment.**

1. Introduction

Transparent conducting oxides (TCOs) are a group of metallic oxides like ZnO, CdO, In_2O_3, SnO_2 and Ga_2O_3 that have many industrial applications, especially in optoelectronics [1]. Their optical and electrical properties could be controlled by means of their natural structural point defects. One of the methods by which we can control their structural defects is doping with foreign metallic ions. It was found experimentally that doping of TCOs with some metallic ions could increase the concentration of carriers and/or improve the conductivity [2]. Besides, the doping process could generate extra exotic properties in TCOs, such as magnetic, optical or mechanical properties, that could widen the fields of their applications. The present study focuses on doping of CdO for developing conditions necessary to create stable room-temperature ferromagnets (RT-FMs) for applications in the field of dilute magnetic semiconductors (DMSs). To achieve this purpose, it is essential to dope CdO with some transition or rare-earth ions, which have intrinsic magnetic moments. Furthermore, it is required to think about developing the electronic medium in the host crystal (CdO) that is necessary to hold the spin–spin (***S.S***) exchange long-range interaction between localised spins of the dopant ions.

Indeed, more theoretical and experimental works are required to clarify and explain the mechanism by which RT-FM could be created in DMS materials with tiny doping level or even, sometimes, without doping. Some researchers attribute the creation of RT-FM in undoped oxides to their intrinsic point defects, such as oxygen (O) vacancies [3–5]. However, the role of O-vacancies in creating/boosting RT-FM is still under study.

In the present work, dopants Co^{2+} magnetic ions are used as a source of stable FM in CdO. It is known that the magnetic moment of Co^{2+} ion is 4.2−4.8 μ_B (where μ_B is Bohr magneton) as measured experimentally in some tetrahedral complexes [6]. In addition, some facts related to the doping process should be mentioned: the VI-coordination ionic radius of Cd^{2+} (0.095 nm) is close to that of Co^{2+} (0.0745 nm) [7] and the crystalline structures of CdO and CoO are identical (rock-salt Fm-3m). Therefore, high solubility of Co^{2+} ions in CdO is expected, forming substitutional solid solution (SSS). Furthermore, the In^{3+} ionic radius (0.08 nm, coordination VI) [7] is less than that of Cd^{2+}, which permits In^{3+} ions to occupy the positions of Cd^{2+} ions in CdO crystal without disturbing the crystalline structure.

Several usual chemical and physical methods are used to synthesise metal-doped CdO powder; however, in the present work, pure and doped CdO powders were synthesised by means of thermal decomposition of Cd chloride

*Author for correspondence (adakhil@uob.edu.bh)

[$CdCl_2 \cdot H_2O$]. Moreover, the synthesis procedure involved using dilute HCl acid.

Cobalt ions were used as a dopant to many oxides, like SnO_2 [8] or In_2O_3 [9] in order to study their magnetic properties, where paramagnets with weak antiferromagnetism (AFM) interactions were observed. Paramagnetic (PM) behaviour was observed in Co-doped CdO powder prepared by thermal decomposition of organic complexes [10]. Moreover, weak AFM superimposed on major PM properties was observed at low temperatures (5 K) in Co-doped CdO system [11]. However, FM behaviour was observed in Co-doped ZnO powder, which was explained by the presence of oxygen vacancies and zinc interstitials [12]. Thus the created magnetic behaviour qualitatively depends on the kind of dopants and host, and the details of the used procedure of synthesis.

2. Experimental

Nanoparticle solid solution powders of Co–In-codoped CdO have been synthesised by solvothermal method through $CdCl_2 \cdot H_2O$ precursor route. Pure Cd, In and Co fine powders of analytical grade (supplied from Sigma-Aldrich products) and HCl were used as starting materials in order to synthesise pure and Co–In-codoped cadmium chloride ($CdCl_2 \cdot H_2O$) precursor powder. The procedure of synthesise is quite simple. A mixture of controlled amounts of Cd, In and Co fine powders was dissolved in dilute (∼3%) HCl acid under continuous mild magnetic stirring at RT for ∼24 h, until the solution color changed to that of fat milk. Finally, the suspended white precipitate was collected by slow evaporation at 80°C. The produced precipitate powder was flash calcined in a closed oven at 500°C for 1 h followed by natural cooling to room temperature. The yielded white precursor powder was tested by the X-ray diffraction (XRD) method, which established that it had just the $CdCl_2 \cdot H_2O$ structure. Next, the synthesised precursor powder was thermally decomposed by calcination at ∼800°C for ∼2 h in order to obtain the final product of CdO crystalline structure product. It must be mentioned here that by thermochemistry analysis it was found [13] that during the decomposition of $CdCl_2 \cdot H_2O$ to CdO, it lost 61% of its weight by volatilisation.

Two concentrations of cobalt dopant were prepared. The ratios Co/Cd were 10 at% for the CdO:Co–In (S1) sample and 30 at% for sample CdO:Co–In (S2), while only one In/Cd concentration ratio of 3 at% was used in both samples. Finally, some amount of the final as-synthesised CdO product powder was post-annealed in hydrogen atmosphere at 350°C for 30 min.

The elemental analysis of the samples was performed by the X-ray fluorescence (XRF) method. The structural analysis of the samples was carried out using a Rigaku Ultima *VI* θ–2θ X-ray diffractometer with Cu K_α rays. The optical properties of the prepared powder samples were studied by diffuse reflectance spectroscopy (DRS). The magnetic properties were measured with a Micro-Mag Model 3900.

3. Results and discussion

3.1 *Structural analysis*

The XRF spectra of the synthesised final host CdO samples S1 and S2 are depicted in figure 1. The spectra disclose the elemental contents and, hence, the purity of the synthesised powders. They show Cd L-spectrum (3.13–3.53 keV) and Co K_α and K_β signals (6.93 and 7.65 keV, respectively), and the

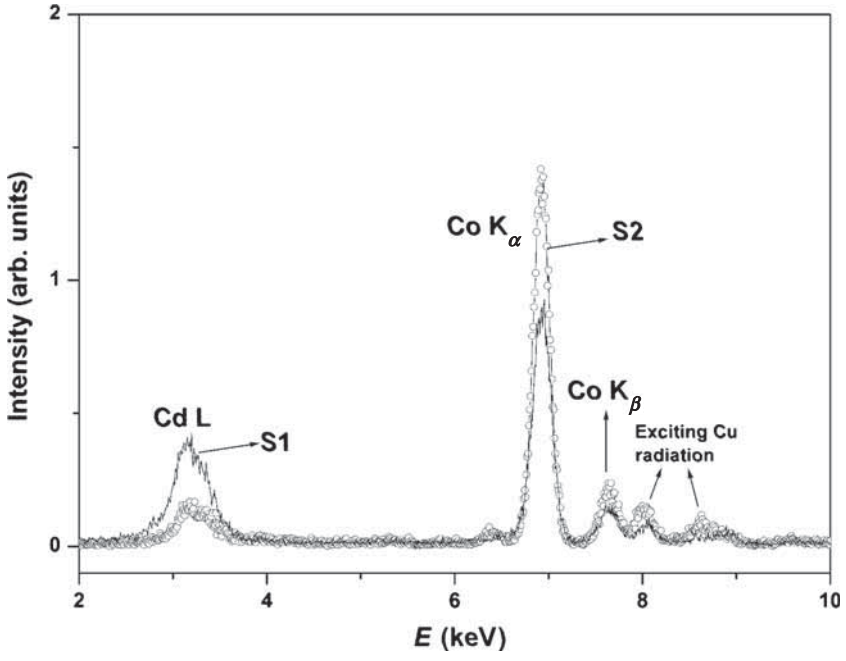

Figure 1. XRF spectra of the prepared powder S1 and S2 samples.

exciting Cu K_α and K_β signals (8.04 and 8.90 keV, respectively). The In signal (3.28 keV) completely overlapped with the Cd L-spectrum due to the small content of In. No additional XRF signals were detected, indicating to the elemental content and purity of the prepared samples.

Figure 2 shows the XRD patterns of the precursor powders. They were indexed according to the crystalline structure of cadmium chloride hydrate ($CdCl_2{\cdot}H_2O$), which is principally formed by the well-known chemical reaction $CdO + 2HCl \rightarrow CdCl_2 + H_2O$. The crystalline structure of $CdCl_2{\cdot}H_2O$ is known to be orthorhombic Pnam (62) with parameters $a = 0.92610$ nm, $b = 1.17300$ nm, $c = 0.37940$ nm and $V_{cell} = 0.412.148$ nm^3 [14]. In the present work, the refinement parameters by the Rietveld method for the precursor powders of undoped and Co–In-codoped CdO powders are given in table 1. The results prove the total incorporation of In^{3+} and Co^{2+} ions in the lattice of the synthesised solid precursors. Also, the XRD data reveal that the prepared $CdCl_2{\cdot}H_2O$ precursors are nanocrystallite powders.

The XRD of final synthesised powders is shown in figure 3. The patterns reveal that the synthesised powders are polycrystalline CdO in cubic structure. The absence of diffraction peaks arising from pure or related Co/In phases refers to the incorporation of Co^{2+}/In^{3+} ions in the lattice of host CdO, forming S1 and S2 solid solutions. The results of the structural analysis: lattice parameter (calculated by Rietveld crystal refinement), crystallite size (CS) and strain (calculated by the Halder–Wagner method), are listed in table 2.

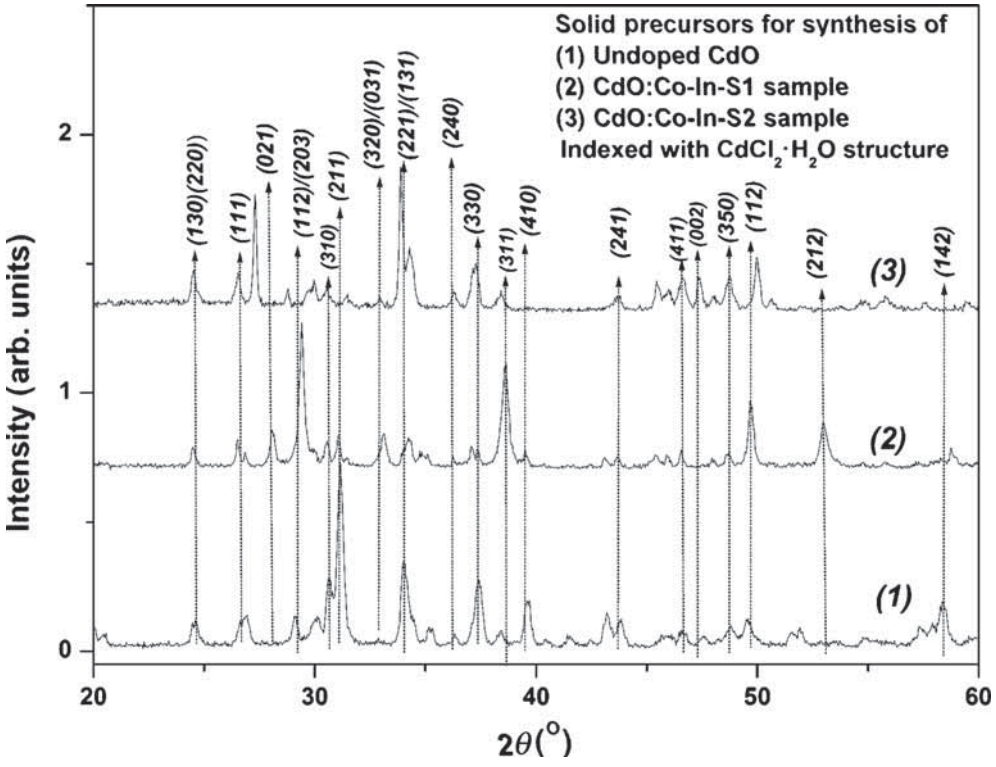

Figure 2. XRD patterns of the precursor powders for syntheses of undoped CdO, S1 and S2 samples.

Table 1. Structural analysis: crystallite size (CS), micro-strain, lattice parameters (a, b and c, V_{cell}) and Rietveld refinement quality parameters for precursor powders of synthesis of CdO, S1 and S2 samples.

Sample	CS (nm)	Strain (%)	Lattice parameters (Å)	Refinement factors					
				V_{cell} (Å^3)	R_{wp} (%)	R_p (%)	R_e (%)	S	χ^2
Precursor of undoped CdO	20.7	0.15	$a = 9.253$ $b = 11.735$ $c = 3.790$	411.5	39.37	30.95	13.23	2.9764	8.8592
Precursor of CdO:Co–In-S1	23.7	0.18	$a = 9.259$ $b = 11.729$ $c = 3.7916$	411.7	25.08	18.57	16.5	1.5186	2.3061
Precursor of CdO:Co–In-S2	21.4	0.10	$a = 9.251$ $b = 11.727$ $c = 3.793$	411.5	33.78	24.58	14.76	2.2888	5.2388

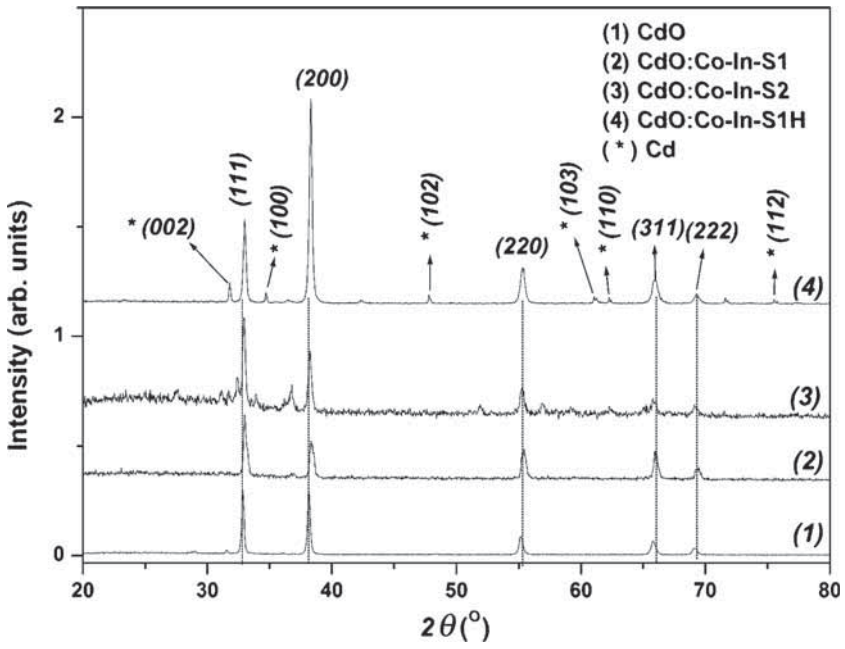

Figure 3. XRD patterns of samples CdO, S1, S2 and S1-H powders.

Table 2. Structural analysis: crystallite size (CS), the structural micro-strain, lattice parameter (a), Rietveld refinement quality parameters and optical bandgap (E_g (eV)).

Sample	CS (nm)	Strain (%)	Lattice parameter a (Å)	Refinement factors					
				R_{wp} (%)	R_p (%)	R_e (%)	S	χ^2	E_g
CdO	73.2	0.26	4.7044	16.98	13.65	11.4	1.487	2.211	2.1
CdO:Co–In-S1	25.9	0.21	4.6927	17.37	13.73	15.15	1.144	1.310	2.05
CdO:Co–In-S1H	66.7	0.32	4.6961	36.81	29.92	11.96	3.072	9.437	2.90
Cd (16.7%)	42.8	0.09	$a = 2.9802$, $c = 5.6190$	25.08	21.16	211.91	2.101	4.417	
CdO:Co–In-S2	40.6	0.23	4.702	16.96	12.87	11.81	1.434	2.057	1.90

The lattice constant of undoped CdO powder was found to be close to the value given in JCPDS Card No. 05-0640 (Fm-3m, $a = 0.4695$ nm) (JCPDS File No. 05-0640). However, the volume of the unit cell ($V_{cell} = a^3$) of host CdO slightly reduced, comparing with undoped CdO, due to the doping by Co^{2+}/In^{3+} ions of slightly smaller ionic radius than that of Cd^{2+}. The monophase of S2 with high Co doping level shows that cobalt ions have high solubility in CdO. The substitution of Cd^{2+} ions by Co^{2+} ions would not strongly disturb the crystalline structure and did not disturb the charge neutrality of the unit cell. Therefore, the substitution for Cd^{2+} ions by Co^{2+} ions is the most likely to occur, forming SSS in addition to the possible occupation by Co^{2+} of some interstitial positions in CdO structure. However, the occupation of Cd^{2+} positions by In^{3+} ions disturbs the charge neutrality of the unit cell, which would be settled by redistribution of ions in the unit cell. The XRD pattern of hydrogenated S1 sample (i.e., S1H) is shown in figure 3, which reveals two major structural modifications. First, extra weak peaks appear in the XRD pattern, which are attributed to the formation of Cd metal nanograins. The XRD results for the liberated Cd grains given in table 2 confirm that they are of nano-size with hexagonal structure and parameters $a = 0.29802$ nm and $c = 0.56190$ nm, which are close to the previously known HCP ($P6_3/mmc$) structure with lattice parameters $a = 0.29794$ nm and $c = 0.56186$ nm [15]. The liberated Cd ions are due to the interaction between hydrogen and structural oxygen ions that leads to their removal from the host CdO crystalline structure, forming oxygen vacancies (V_O). The removal of structural oxygen ions disturbs the electro-neutrality of the host CdO unit cell that would be settled by liberation of Cd ions outside the host CdO lattice.

Due to the liberation and expelling of Cd ions, the lattice imperfection/strain increased by about 1.5 times (table 2). Furthermore, the highest peak intensity position changed from (111) in S1 to (200) in S1H (figure 3). Another observation is that the CS considerably grew by about 2.5 times (table 2). This might be explained by the movement of

the ions by hydrogen impacts that increases the agglomerations on crystallites or gradual removal of the crystallite boundaries. The reduction of oxygen content increases the unit cell volume (V_{cell}), which is clearly observed in data of table 2. Such observation was also previously mentioned in Refs. [16,17].

To completely understand the effect of hydrogenation, it should be mentioned that H_2 molecules might be dissociated into H atoms on the surface of nanocrystallites and nanograins due to the presence of Co ions, playing a role of catalyst since the transition metals (TMs) are well known to possess high catalytic effect for H_2 molecules dissociation [18,19]. Later, the H atoms will be adsorbed at the surface of nanoparticles and diffuse into the bulk through interstitial sites or vacancies within CdO crystal lattice followed by interaction with structural oxygen, forming oxygen vacancies and thus boosting the magnetic properties [20]. Therefore, it should be expected that sample S1H must have stronger FM properties than those of S1. It should be mentioned that this effect did not happen with pure undoped CdO; it must need a metallic catalyst like TM ions to be involved. Therefore, as a general conclusion, hydrogenation of TM-doped CdO would produce a nanocomposite crystal consisting of Cd nanoparticles immersed in TM-doped CdO crystalline solid medium.

3.2 *Optical properties*

The optical properties of the synthesised powders were studied by the DRS method. The spectral diffuse reflectance $R(\lambda)$ was measured in the range 250–900 nm relative to the standard reference reflectance (R_{BaSO_4}) from a $BaSO_4$ powder supplied by Schemadzu, i.e., $R(\lambda) = R_{sample}/R_{BaSO_4}$, and the results are shown in the inset of figure 4. These R-spectra are usually used to estimate the bandgap of the powders using the Kubelka–Munk (K-M) equation [21]

$$K/S = F(R) = (1 - R)^2/2R, \tag{1}$$

where $F(R)$ is called as the K–M function, S is the scattering coefficient and K is called as the K–M absorption coefficient, where $K = 2\alpha$ and α is the absorption coefficient. Considering S as a constant with respect to the wavelength (λ), it is possible to use $F(R)$ in the well-known Tauc plot technique in order to estimate the direct E_g, i.e., the extrapolation of the linear portion of $[F(R) \times E]^2$ *vs.* E plot, as shown in figure 4. The obtained direct bandgaps are given in table 2. The bandgap found for undoped synthesised CdO nanopowder is consistent with the known range (2.1–2.6 eV) for undoped CdO films [1]. However, with Co/In incorporation, the bandgap is red-shifted. This result refers to the doping of Co^{2+}/In^{3+} ions in CdO crystalline structure, which creates an impurity band at the tail of conduction band. The impurity band becomes wider with increasing Co doping level, which means larger decrease in E_g, as given in table 2. This result is in agreement with Ref. [22]. Moreover, the hydrogenation blue-shifts the bandgap (table 2). Increase of bandgap (E_g) with hydrogenation could be explained by the Moss–Burstein effect [23]; i.e., E_g increases with increasing concentration of free carriers (n_{el}). Thus, the hydrogenation of semiconducting oxide CdO at relatively low temperature (350°C) and for a short time period (30 min) is beneficial for generation of more free electrons, which might improve the electronic crystalline medium for boosting the spin–spin (***S.S***) interaction.

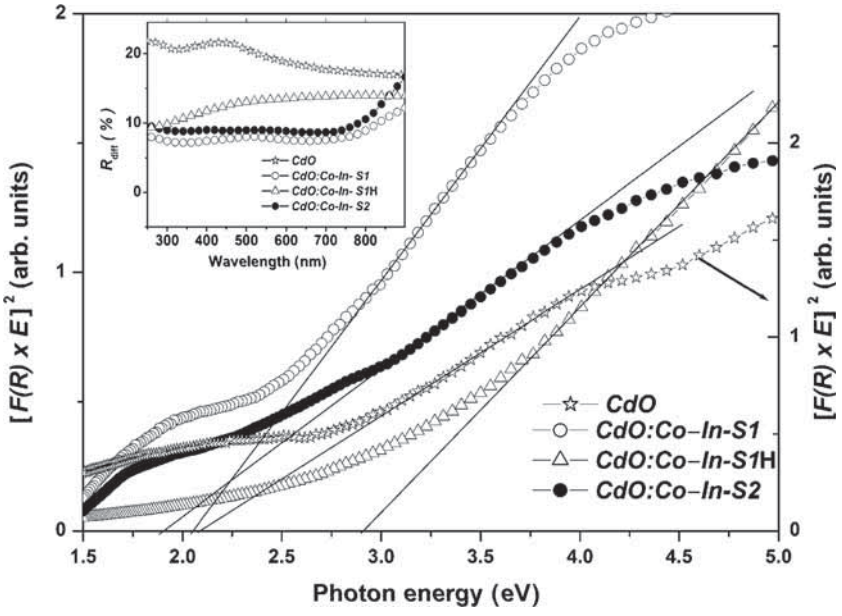

Figure 4. Tauc plot for the samples CdO, S1 and S1-H. The inset shows spectral diffuse reflectance for CdO, S1 and S1-H powders.

3.3 *Magnetic properties*

It is known that undoped, bulk and stoichiometric CdO powder has diamagnetic (DM) properties at RT [24]. However, it was observed that structural point defects like vacancies could create in CdO a very weak FM component superimposed on the main DM characteristics (i.e., DM+FM) [25]. However, for practical applications in DMS, it is necessary to create stable and considerable FM properties from spin–spin (***S.S***) exchange interaction between dopant ions. However, the realisation of ***S.S*** exchange interaction depends on the interionic exchange distances (R) and the properties of electronic medium of host crystal (CdO) through which the ***S.S*** interaction takes place. Generally, it was established that the ***S.S*** exchange interaction requires $R \leq 1.5a$, where a is the lattice parameter of host medium [26]. R could be estimated as radius of a sphere around each Co^{2+} ion. For a uniform distribution of Co^{2+} dopants within the host CdO, the value of R can be estimated by the relation $n_{Co}V = 1$, where n_{Co} is the dopant Co^{2+} concentration and $V = (4/3)\pi R^3$. Thus, the relative ionic concentration of dopant Co^{2+} to host Cd^{2+} should obey the relation $(n_{Co}/n_{Cd}) \geq 1.8\%$ in order to switch on the ***S.S*** exchange interaction. This condition is followed in the present work, which means that FM interaction should be present for a suitable electronic interaction medium, which can be controlled by the experimental details and conditions.

In the present work, FM properties were generated in CdO nanocrystallite powder synthesised from Cd chloride ($CdCl_2{\cdot}H_2O$) by means of Co/In-codoping (sample S1), as shown in figure 5. The FM parameters: coercive force (H_c), remanence (M_r) and saturation magnetisation (M_s) of S1, are given in table 3, where the power product $U_m = H_c M_r$ was introduced as a measure for FM figure of merit [27]. The U_m value for sample S1 is small, indicating weakly generated FM properties.

From basic principles, it is possible to boost the created FM properties in the sample S1 either by enhancing the strength of the spin–spin (***S.S***) interaction between the dopant Co^{2+} ions or by increasing the concentration of spins (***S***) participating in mutual ***S.S*** interaction, i.e., by increasing the Co-doping level. The first approach could be realised by enhancing the internal crystalline electronic medium ***S.S*** interaction through hydrogenation method. In the present work we would like to compare and discuss these two approaches for the enhancement of the created FM.

Figure 5 and table 3 present the experimental magnetic results for samples S1, S2 and S1H. Data show that the hydrogenation of sample S1 strongly boosts its magnetic

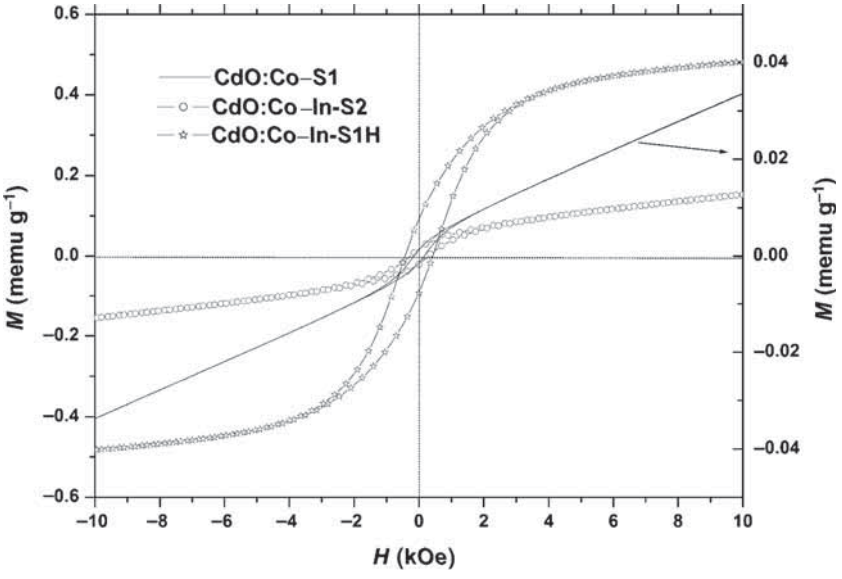

Figure 5. Experimental results of M–H dependence of the samples S1, S2 and S1-H.

Table 3. Obtained values for the coercivity (H_c), remanence (M_r), saturation magnetisation (M_s) and energy product ($U_m = H_c M_r$) for the samples.

Sample	H_c (Oe)	M_r (memu g^{-1})	M_s (memu g^{-1})	$U_m = H_c M_r$ (erg)
CdO	90	0.16	1.1	0.014
CdO:Co–In-S1	232.9	1.42	4.44	0.331
CdO:Co–In-S1H	442.7	93.23	401.7	41.3
CdO:Co–In-S2	307.2	20.1	65.5	6.2

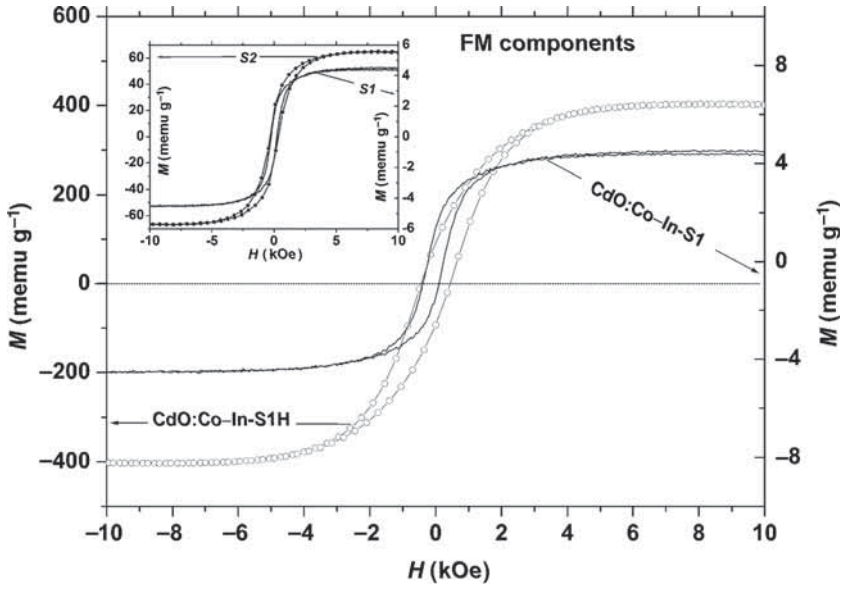

Figure 6. Comparison plot for the effect of hydrogenation on the hysteresis loop of S1. The inset shows a comparison plot for the effect of Co doping level on the hysteresis loops of S1 and S2 samples.

properties, more than that with S1 by increasing the dopant cobalt ions concentration; for example the saturation magnetisation was enhanced ∼14 times with increasing of dopant Co ions concentration while it was enhanced ∼90 times by hydrogenation means. This reflects the essential importance of the electronic medium necessary for the ***S.S*** interaction. Figure 6 shows a schematic comparison between the enhancements of the hysteresis loop (FM component) by the above-mentioned two means.

It becomes known that the hydrogenation induces some structural and electronic variations, which control the properties of the electronic medium in host CdO crystal responsible for the ***S.S*** interaction and, thus, boosts the generated FM. The structural study reveals the interaction between hydrogen atoms and structural oxygen in Cd oxide lattice and, thus, creates oxygen vacancies (V_O) with liberation of free Cd ions of different amounts depending on hydrogenation conditions (time and temperature). The O-vacancies supply/enhance magnetic medium for ***S.S*** interaction and, thus, generate/boost FM. Therefore, the enhancing of FM properties with hydrogenation is a direct proof that O-vacancies (V_O) supply a medium for the ***S.S*** interaction and thus enhance the FM properties. According to the principles of bound magnetic polaron (BMP) theory [28,29], the O-vacancies bind some electrons (polarons) through which the ***S.S*** exchange interaction couples the Co-$3d^7$ ions, causing long-range FM ordering. The strength of the ***S.S*** exchange interaction depends on the number density of polarons and O-vacancies, which could be controlled by the doping process and details of preparation and synthesis.

Figure 5 shows that in the field region $B > 3$ kOe, the magnetisation (M) of both S1 and S2 powders is due to superimposed saturation magnetisation (M_s) of the FM contribution and PM contribution, i.e., the variation in $M(H)$ is due to PM contribution. Therefore, the slope of the straight line for $H > 3$ kOe gives the PM contribution susceptibility:

$$M(H) = M_s + \chi_m H, \quad H > 3 \text{ kOe}. \tag{2}$$

The concentration of the active dopant ions interacting paramagnetically with the applied field (n_{ion}) can be estimated by the Curie equation for volume susceptibility $\chi_{(vol)}$ in cgs units:

$$\chi_{(vol)} = n_{ion}\mu^2/3k_BT, \tag{3}$$

where μ is the magnetic moment per dopant ion, k_B is the Boltzmann constant and T is the working temperature. From the straight-line portion (for $H > 3$ kOe) of M–H graph in figure 5, $\chi_m = 2.94 \times 10^{-6}$ emu (g Oe)$^{-1}$ for S1 sample and $\chi_m = 9.21 \times 10^{-6}$ emu (g Oe)$^{-1}$ for S2 sample. Using $\mu_{(Co)} = 4.2\ \mu_B$, the relative concentration of magnetically active Co^{2+} ions is ∼50% for S1 and ∼53% for S2. In general, not all dopant Co^{2+} ions participate in the magnetic responses. This might be due to the medium bonds, constrains, distribution or location of ions [30,31].

4. Conclusions

Nanoparticle powders of solid solution $Cd_{1-x-y}In_yCo_xO$ (x = 0, 0.10 and 0.40, $y = 0.03$) have been synthesised by the solvothermal method through cadmium chloride ($CdCl_2 \cdot H_2O$) precursor route. The structural study showed that the precursor $CdCl_2 \cdot H_2O$ has an orthorhombic (Pnam) structure. The incorporated Co/In ions were totally doped in the final product CdO lattice. The investigation confirms that the

hydrogenation of Co–In-codoped CdO solid solution sample liberates Cd metal and induces oxygen vacancies, which boosts the FM properties of the sample. Such a phenomenon cannot happen without the presence of transition metal cobalt playing a role of catalyst. Therefore, as a general important conclusion, hydrogenation of TM-doped CdO would produce a nanocomposite crystal consisting of Cd nanoparticles immersed in TM-doped CdO crystalline solid medium.

The optical study showed red-shift of host CdO bandgap due to Co/In doping and blue-shift with hydrogenation, which is related to a strong structural change. The magnetic investigations show that doping of CdO with Co^{2+}/In^{3+} ions creates RT-FM, which strongly boosted with hydrogenation, so that H_c enhanced ∼2 times, B_r ∼65 times and B_{sat} ∼90 times. In general, the results demonstrate the significant importance of the electronic medium through which $\boldsymbol{S}.\boldsymbol{S}$ interaction takes place. The results of the present work demonstrate a potential candidate medium consisting of free Cd nanoparticles immersed in Co–In-codoped CdO for future DMS applications.

References

[1] Zhao Z, Morel D L and Ferekides C S 2002 *Thin Solid Films* **413** 203

[2] Dakhel A A 2012 *J. Electr. Mater.* **41** 2405

[3] Shaohua Sun, Ping Wu and Pengfei Xing 2012 *J. Magn. Magn. Mater.* **324** 2932

[4] Kohan A F, Ceder G, Morgan D and Van de Walle C G 2000 *Phys. Rev. B* **61** 15027

[5] Choudhury B, Choudhurym A, Maidul Islam A K M, Alagarsmy P and Mukhherjee M 2011 *J. Magn. Magn. Mater.* **323** 440

[6] Lancashire R J 2015 Department of Chemistry, University of West Indies, Jamaica Web: http://wwwchem.uwimona.edu.jm/spectra/MagMom.html

[7] Shannon R D 1976 *Acta Crystallogr. A* **32** 751

[8] Ahmad Tokeer and Khatoon Sarvari 2015 *J. Mater. Res.* **30** 1611

[9] Khatton S, Coolahan K, Lofland E S and Ahmed T 2013 *J. Am. Cer. Soc.* **96** 2544

[10] Dakhel A A and Bououdina M 2014 *J. Supercond. Nov. Magn.* **27** 2507

[11] Ahmad T, Khatoon S, Lofland S E and Thakur G S 2014 *Mater. Sci. Semicond. Proc.* **17** 207

[12] Gandhi V, Ganesan R, Syedahamed H H A and Thaiyan M 2014 *J. Phys. Chem. C* **118** 9715

[13] Srivastava O K and Secco E A 1967 *Canadian J. Chem.* **45** 1375

[14] Technisch Physische Dienst 1975 Delft, Netherlands: ICDD Grant-in-Aid JCPDS File No. 05-0640

[15] Edwards D A, Wallace W E and Craig R S 1952 *J. Am. Chem. Soc.* **74** 5256

[16] Yang J, Song W H, Zhang R L, Ma Y Q, Zhao B C, Sheng Z G *et al* 2004 *Solid State Commun.* **131** 393

[17] Dakhel A A, El-Hilo M and Bououdina M 2014 *Adv. Powder Technol.* **25** 1839

[18] Lewis E A, Le D, Murphy C J, Jewell A D, Mattewra M F G, Liriano M L *et al* 2012 *J. Phys. Chem. C* **116** 25868

[19] Pozzo M and Alfe D 2009 *Int. J. Hydrogen Energy* **34** 1922

[20] Schlapbach L 1980 *J. Phys. F: Met. Phys.* **10** 2477

[21] Morales A E, Mora E S and Pal U 2007 *Rev. Mexicana Fis. S* **53** 18

[22] Sahin B, Bayansal F, Yuksel M and Cetinkara H A 2014 *Mater. Sci. Semicond. Proc.* **18** 135

[23] Burstein E 1954 *Phys. Rev.* **93** 632

[24] Chandiramouli R and Jeyaprakash B G 2013 *Solid State Sci.* **16** 102

[25] Bououdina M, Dakhel A A, El-Hilo M, Anjum D H, Kanoun M B and Goumri-Said S 2015 *RSC Adv.* **5** 33233

[26] Seo S Y, Kwak C H, Kim S H, Park S H, Lee I J and Han S W 2012 *J. Cryst. Growth* **346** 56

[27] Raghavan V 2004 *Materials science and engineering: a first course* 5th edn (New Delhi: Prentic-Hall of India Private Limited), p 406

[28] Kaminski A and Sarma S D 2002 *Phys. Rev. Lett.* **88** 247

[29] Wolff P A, Bhatt R N and Durst A C 1996 *J. Appl. Phys.* **79** 51

[30] Cheng Shun-Jen 2005 *Phys. Rev. B* **72** 235332

[31] Tolea F, Grecu M N, Kuncser V, Constantinescu S Gr and Ghica D 2015 *Appl. Phys. Lett.* **106** 142404